ELSEVIER

Chemical Engineering Journal 138 (2008) 602–607

Chemical Engineering Journal

www.elsevier.com/locate/cej

Ethanol steam reforming using Ni(II)-Al(III) layered double hydroxide as catalyst precursor Kinetic study

Mas Verónica, Baronetti Graciela, Amadeo Norma *, Laborde Miguel

Laboratorio de Procesos Catalíticos, Departamento de Ingeniería Química, Facultad de Ingeniería, Universidad de Buenos Aires, Ciudad Universitaria, Pabellón de Industrias (1428), Buenos Aires, Argentina

Received 6 July 2007; received in revised form 14 August 2007; accepted 24 August 2007

Abstract

A preliminary kinetic study of ethanol steam reforming using a Ni(II)-Al(III) lamellar double hydroxide (LDH) as catalyst precursor is carried out within the region of kinetic rate control. Ni(II)Al(III) precursor is synthesized by means of homogeneous precipitation by urea. Under highly diluted feed conditions used in the kinetic experiments, products obtained are H_2, CO, CO_2 and traces of CH_4. A parallel kinetic set is capable to describe the product distribution obtained. Assuming power law, kinetic parameters were fitted for both reactions involved in an operation range where reaction rate was assumed to be independent of water concentration. Ethanol orders were found to be lower than 1. A maximum ethanol conversion was found as a function of water concentration in the feed. Experiences with different methane concentrations showed that ethanol conversion decreases when methane concentration increases. These results reveal the existence of competitiveness between both reactants and methane to be adsorbed in the same type of active site. In order to complete the kinetic study, the Langmuir Hinshelwood model is expected to apply.

Keywords: Hydrogen; Bioethanol; Steam reforming; HDL Ni(II)Al(III); Kinetic

1. Introduction

Hydrogen is a clean energetic vector since feeding into a fuel cell allows the conversion of chemical energy into electric energy. Bioethanol produced by fermentation of sugar cane, corn and other agricultural waste is a very attractive and renewable raw material for the production of hydrogen due to its great content of hydrogen atoms. Furthermore, the use of bioethanol for the production of hydrogen has a beneficial effect from the environmental point of view since it prevents the consumption of fossil fuels. From ethanol steam reforming reaction:

$$C_2H_5OH + 3H_2O \rightarrow 2CO_2 + 6H_2.$$

A theoretical yield of 6 mol H_2 per mol ethanol could be obtained.

Nevertheless, the presence of non-desired reactions might affect hydrogen selectivity. Ethanol steam reforming has been studied using catalysts based in Ni, Co, Ni–Cu and noble metal such as Pd, Ru and Rh [1–6]. From those results it can be seen that the activity and product distribution depend on the type and amount of metal used, the type of support and the method used to prepare it. The major interest is to develop a catalyst that is active and selective to H_2.

Since Ross et al. researching work to current studies [7–12], different methods of preparation and procedures for activating Ni(II)Al(III) hydrotalcite type precursor have been reported with the aim of using it as steam reforming catalyst. The use of Ni(II)-Al(III) lamellar double hydroxides (LDHs) allows to reach an intimate mixture of cations in a crystalline structure and turns them into excellent precursors to obtain mixed oxides in a wide range of composition. Hence, its thermal decomposition leads to oxide amorphous crystalline phases which after being subjected to a posterior reduction are transformed into dispersed metallic phases in an oxidic matrix [13].

In addition, some kinetic studies have been published in which power law [14–16], Eley Rideal-like model [17] and Langmuir Hinshelwood model (over Co-based catalyst) [18], kinetic expressions are reported. It is worth mentioning that

* Corresponding author. Fax: +54 114576 3211.
E-mail address: norma@di.fcen.uba.ar (A. Norma).

1385-8947/$ – see front matter © 2007 Elsevier B.V. All rights reserved.
doi:10.1016/j.cej.2007.08.035

Nomenclature

Conversion	$(y_{\text{ethanol in}} - y_{\text{ethanol out}})/y_{\text{ethanol in}}$
D	reactor inner diameter
D_p	catalyst particle size
E_{a_i}	activation energy of the ith reaction (J/mol)
$F_{\text{total molar}}$	total molar flow in the feed (mol/min)
K_i^0	pre-exponential factor of the kinetic constant
L	catalytic bed height
P_j	partial pressure of the jth component
P	pressure (atm)
r_i	ith reaction rate (mol/min mg)
R	ideal gas constant (8.314 J/mol K)
T	temperature (K)
y_j	molar ratio of the jth component
Yield of the jth product	$y_j/y_{\text{ethanol in}}$

Greek letters

θ	space time (min mg/mol)
ω	catalyst mass (mg)

since this catalytic reaction is a fluid/solid heterogenic process and decomposition rate of ethanol happens at high rate, the reaction is bound to be influenced by heat transfer as well as pore and boundary layer mass diffusion. This might explain the large discrepancy and low activation energy values reported.

The goal of this study is to carry out a systematic study of kinetic variables (concentration, temperature and catalyst mass) present in the steam reforming of ethanol using Ni(II)-Al(III) LDH as precursor and thus to fit a simple power law kinetic expression.

2. Experimental methods

2.1. Catalyst preparation

Catalyst precursor has been synthesized by urea method, aging mixed solutions containing nickel(II)-aluminium(III) and urea. Details of the procedure are provided elsewhere [19].

Activation of the precursor was carried out by reduction with pure hydrogen during 2 h with a ramp rate of 10 K min^{-1} to reach the activation temperature of 923 K.

2.2. Catalyst characterization

Ni(II)-Al(III) LDH was characterized by X-ray diffraction (XRD) and temperature programmed reduction (TPR). Fresh and reduced solid were characterized by XDR in a Siemens D 5000 (Cu Kα radiation) equipment for 2θ in a range 5–70°.

TPR experiments were carried out using a quartz reactor placed in an electric oven. Thirty milligrams of sample were used and 100 ml min^{-1} of N_2/H_2 (98/2 mol%) with a ramp of 5 K min^{-1} in a range 293–1173 K.

2.3. Catalytic reaction

Catalytic evaluation was performed in a quartz reactor of 4 mm i.d., placed in the interior of an electric oven. Reactor temperature was controlled to attained isothermal conditions by means of a slid thermocouple placed inside the catalytic bed. Reactants, consisting of an ethanol and water mixture, were fed with a HPLC-like syringe pump. The mixture was evaporated, in 20 ml/min stream of N_2, in an electric oven at 623 K and subsequently diluted with a stream of 335 ml/min of argon shortly before entering the reactor. With the aim of preventing pore diffusion effects, the catalyst was ground to diameter range 44–88 μm, and inert material of the same size was used to prevent temperature gradient inside the catalytic bed. Liquid flow was varied in a range $(1.32–6.8) \times 10^{-2}$ ml min^{-1}, while water/ethanol molar ratio in the feed ranging from 3.5 to 10. The catalyst was analyzed in a temperature range from 823 to 923 K and space time $(1.2–6.2) \times 10^{-4}$ g min mol^{-1}, calculated as the catalyst mass in grams per total molar flow in mol min^{-1}.

The feed and effluent pipes were heated to avoid any condensation. Stainless steel pipe was used with the aim of avoiding ethanol decomposition out of the catalytic bed. Previous to the catalytic evaluation experiments were carried out in order to verify negligible contribution of homogeneous phase reaction and absence of external and internal diffusion limitations. With the aim of ensuring absence of pore diffusion resistance, an experiment using diameter particle smaller than 44 μm was carried out, while all other variables remained constant. In the same way, to make certain that no external diffusion was limiting the rate of reaction, total gas flow was increased. These experiments were all conducted at the highest temperature (923 K) and no significant change in conversion was observed. The plug flow condition was achieved by providing $L/D_p \geq 50$ and $D/D_p \geq 30$ [20]. In all runs the carbon balance closed around 95%, therefore no carbon deposition was verified during typical runs of 10 h.

3. Results and discussion

In Fig. 1a, the pattern of X-ray diffraction (XRD) for the Ni(II)-Al(III) precursor sample is shown. The characteristic

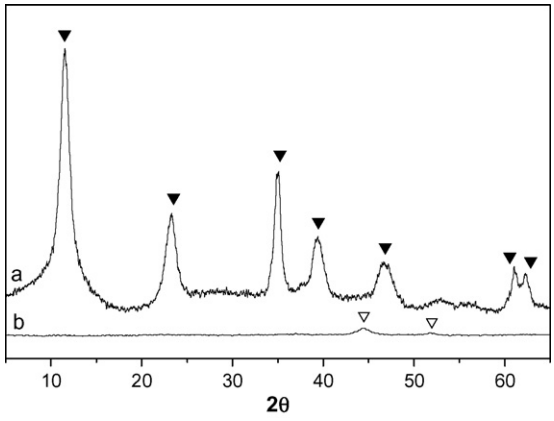

Fig. 1. XDR patterns of: (a) Ni(II)Al(III) precursor sample. (b) NiAl reduced sample.

reflections of the interbasal planes (0 0 3), (0 0 6), (0 1 2), (0 1 5) and (0 1 8) of a crystalline LDH can be seen (Fig. 1a▼). Likewise, the typical doublet of d(1 1 0)–d(1 1 3) planes of LDH can be clearly observed in the zone close to $2\theta = 60–62^{\circ}$. On the other hand, no signals of other crystalline phases are detected.

The XDR pattern of the NiAl reduced sample is shown in Fig. 1b. The low intensity of the signals corresponding to metallic Ni reflections should be noted. According to the Scherrer equation, the mean size of Ni crystals was estimated to be around 5 nm. The Ni particle size has an impact on the nucleation of carbon, responsible of catalyst deactivation, particularly it has been published that smaller the crystal, more difficult is the initiation of carbon formation [21].

The reduction profile obtained for the fresh sample at programmed temperature indicates (Fig. 2) that reduction occurs in a wide range of temperatures associated with the NiAl LDH oxidic forms presented in the sample. The maximum amount of hydrogen consumed was found at 750 K. From these results, a kinetic study of the ethanol steam reforming was performed using NiAl LDH reduced precursor as it was described above. Temperature, space time, ethanol and water concentration were varied systematically, always operating below 100% ethanol conversion in order to obtain experimental data which allowed to carry out the kinetic study. Experiments were conducted under such diluted conditions (8.8/1.6/89.6, water/ethanol/argon average molar ratio) so that the variation in molar number due to the stoichiometry of the reaction could be neglected. In this sense N_2 was used as reference compound in order to verify this behavior. Experiments at different molar fractions in the feed were carried out at the same space time adjusting the inert flow and mass of catalyst. Ethanol conversion and yield of H_2 as function of space time for different temperatures are shown in Figs. 3 and 4, respectively. Continuous lines in all cases show results obtained by simulation with the kinetic parameters fitted. The ethanol conversion and H_2 production increase with temperature and space time. It can be noted that when ethanol conversion approaches to 100%, yield of H_2 approximates to 5. This value is considerably high since the stoichiometric value is 6. The products obtained apart from H_2 are CO_2, CO and

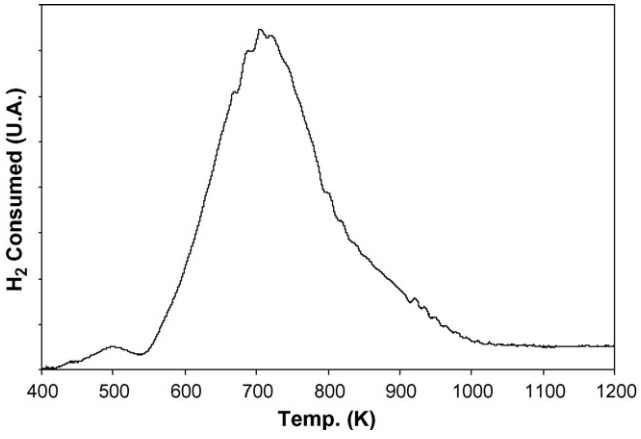

Fig. 2. Programmed reduction temperature profile of Ni(II)Al(III) precursor sample.

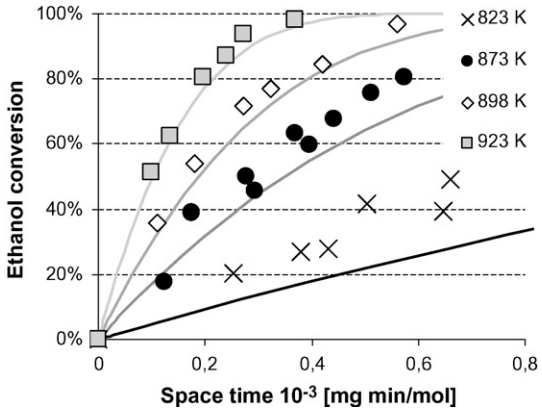

Fig. 3. Ethanol conversion vs. space time at different temperatures.

traces of CH_4 (in all cases CH_4 molar fraction was smaller than 3.2E−4). Typical values of C, H and O balance error in all cases were found to be lower than 5%.

There is strong evidence from previous studies carried out at different temperatures and space time and higher ethanol concentration values [22], to suggest the following set of reactions:

$$C_2H_5OH \rightarrow C_2H_4O + H_2 \quad (1)$$

$$C_2H_5OH \rightarrow C_2H_4 + H_2O \quad (2)$$

$$C_2H_4O \rightarrow CO + CH_4 \quad (3)$$

$$C_2H_4O + H_2O \rightarrow CO_2 + CH_4 + H_2 \quad (4)$$

$$C_2H_4 + H_2O \rightarrow CO + CH_4 + H_2 \quad (5)$$

$$C_2H_4 + 2H_2O \rightarrow CO_2 + CH_4 + 2H_2 \quad (6)$$

However, under the experimental conditions used in this work, reactions (3) and (4) are much faster than reaction (1) and this leads to absence of acetaldehyde in the effluent within the whole range of space time. In the same way, ethylene consume from reactions (5) and (6) seams to be as fast as its generation through reaction (2). Since acetaldehyde and ethylene are strictly intermediate products [22,23] not likely to be found in the effluent at any actual operation condition, the reaction system can be represented as:

$$C_2H_5OH \rightarrow CO + CH_4 + H_2 \quad (7)$$

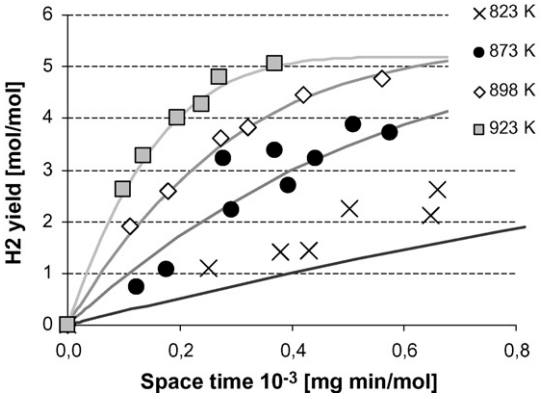

Fig. 4. H_2 yields as a function of space time at different temperatures.

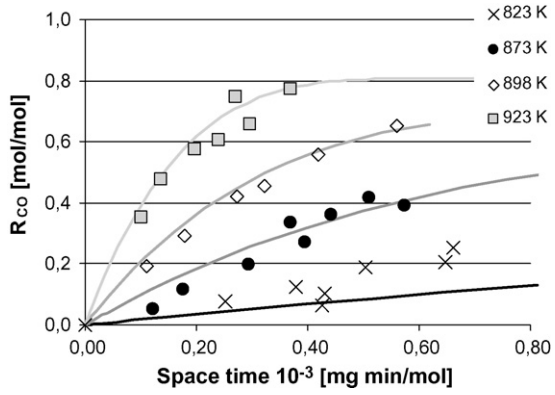

Fig. 5. CO yields vs. space time at different temperatures.

$$C_2H_5OH + H_2O \rightarrow CO_2 + CH_4 + 2H_2 \quad (8)$$

$$CH_4 + H_2O \rightleftarrows CO + 3H_2 \quad (9)$$

$$CH_4 + 2H_2O \rightleftarrows CO_2 + 4H_2 \quad (10)$$

On the other hand, the presence of inert shifts the equilibrium towards products for the methane steam reforming (reactions (9) and (10)), which are known to determine the product distribution [22,24]. Notwithstanding, methane behaves as an intermediate and final product. Traces of methane obtained at any space time give evidence on faster consumption of methane than its production through reactions (7) and (8). Thus, under these operating conditions, rates of reactions (7) and (9) as well as reactions (8) and (10) are strongly correlated and experiments adding methane to the feed should be conducted to break this correlation.

Additionally, CO and CO_2 yield as a function of space time are shown in Figs. 5 and 6. Continuous increase of both yields with space time led to the conclusion that both products can be obtained from a parallel set of reactions. Thus original set of reactions (1)–(6) could be represented by:

$$C_2H_5OH + H_2O \rightarrow 2CO + 4H_2 \quad (11)$$

$$C_2H_5OH + 3H_2O \rightarrow 2CO_2 + 6H_2 \quad (12)$$

Ethanol conversion as a function of water molar feed fraction is shown in Fig. 7 for a constant ethanol molar fraction. It can be noted that ethanol conversion is maximum, which implies that

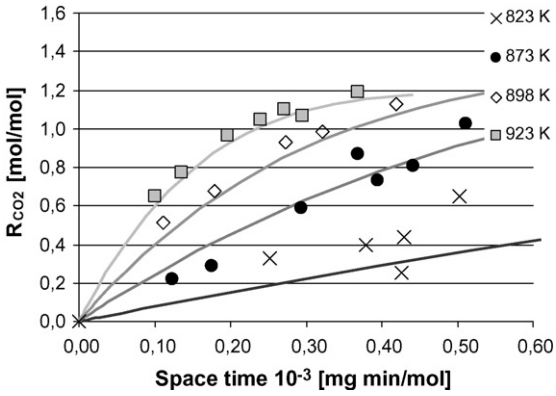

Fig. 6. CO_2 yields vs. space time at different temperatures.

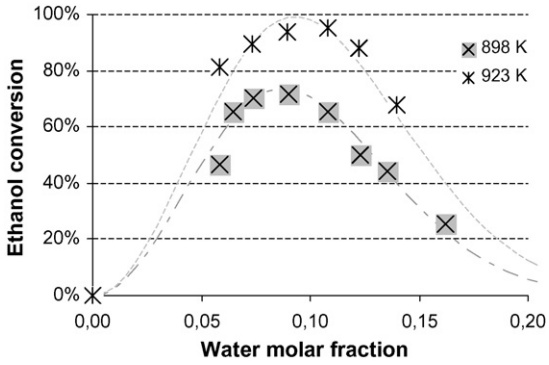

Fig. 7. Ethanol conversion as a function of water molar fraction at 898 and 923 K and space time 2.7×10^{-4} g min/mol.

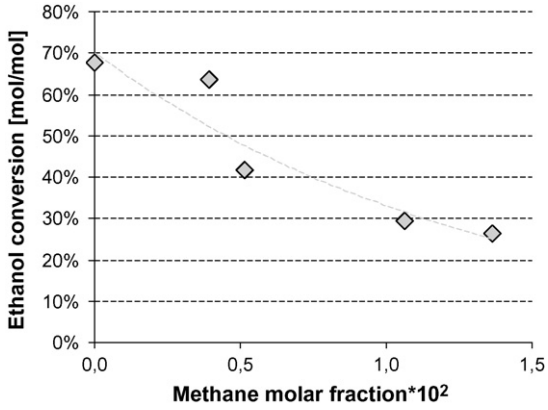

Fig. 8. Ethanol conversion at 898 K as function of methane molar fraction.

ethanol and water are competitively adsorbed on the same active sites. The maximum conversion is reached at ethanol molar ratio of around 5 at 898 K.

In addition, experiments adding methane to the feed were carried out and conversion of ethanol as function of inlet methane molar fraction is shown in Fig. 8. In these experiments CH_4/ethanol/water molar ratios were varied from 0.25/1/5.5 to 0.8/1/5.5. Ethanol conversion drops when methane concentration in the inlet increases suggesting that methane is also adsorbed on the same active sites competing with both ethanol and water. Xu and Froment [25] working on the reforming of methane over a Ni catalyst also found that methane and water compete for the same active site. Rostrup-Nielsen [21] proposed that the support may favor water splitting into OH groups and promote the migration of these reactive species toward the metal particles. According to our results ethanol activation and reaction between hydrocarbon fragments adsorbed and OH occurs on Ni small particles. By virtue of this latter result is that the

Table 1
Estimated kinetic parameters

Parameter	Mean	95% confidence level intervals
K_1^0 (mol/min/mg/atm^n)	5.74E−4	±9.47E−5
E_{a_1} (J/mol)	1.44E+5	±1.29E4
K_2^0 (mol/min/mg/atm^m)	1.88E−4	±1.38E−5
E_{a_2} (J/mol)	2.07E+5	±4.30E4

Table 2
Estimated kinetic parameters according to different authors

Parameter	This work	Other authors			
		Morgenstern et al.	Sun et al.	Akande et al.	Vaidya et al.
E_{a_1} (J/mol)	2.07E+5	1.49E+5	1.87E+3–16.88E+3	4.41E+3	9.6E+4
E_{a_2} (J/mol)	1.44E+5				
T range (K)	823–923	523–573	≈403	593–793	873–973
Ethanol order	0.75–0.8	1	0.43	1	1

Langmuir-Hinshelwood-type reaction mechanism should be formulated for a reliable representation of the kinetic behavior within a wide range of ethanol and water concentration. However, at this stage a power-law-type rate expression was adopted to estimate the value of the kinetic parameters. Reaction rate was assumed to be independent of water concentration, for this reason, experimental data used were those within ethanol/water fed molar ratio ranging from 4.5 to 5.5 since in this range water concentration does not affect the ethanol conversion value.

Considering an isothermal plug flow reactor, the mass balance equations for the reaction system presented above are:

$$\frac{dy_{ethanol}}{d\theta} = -r_{11} - r_{12} \quad (13)$$

$$\frac{dy_{CO}}{d\theta} = 2r_{11} \quad (14)$$

$$\frac{dy_{CO_2}}{d\theta} = 2r_{12} \quad (15)$$

$$\frac{dy_{H_2}}{d\theta} = 4r_{11} + 6r_{12} \quad (16)$$

where:

$$r_{11} = k_{11}^0 \, e^{-(E_{a_{11}}/R)((1/T)-(1/873))} P_{ethanol}^n \quad (17)$$

$$r_{12} = k_{12}^0 \, e^{-(E_{a_{12}}/R)((1/T)-(1/873))} P_{ethanol}^m \quad (18)$$

$$\theta = \frac{w}{F_{total\ molar}} \quad (19)$$

$$P_{ethanol} = P_t y_{ethanol} \quad (20)$$

The kinetic parameters were estimated using the program Athena Visual Workbench. A good fit was found for $n = 0.75$ and $m = 0.8$. In Table 1, the pre-exponential factors, the activation energies and the corresponding confidence intervals are shown for each reaction. In Eqs. (17) and (18) the centered form reduces the correlation between the pre-exponential factor (k^0) and the activation energy (E_a), thereby improving the statistical properties of the estimate for the pre-exponential factor.

Table 2 shows kinetic parameters according to different authors. In spite of the different range of temperature, Morgenstern and Fornango [14] using copper-plated Raney nickel obtained an activation energy very similar to the value obtained in this work. Vaidya and Rodrigues [16], working with a Ru/Al_2O_3 catalyst also found an energy activation value quite similar. On the other hand, Sun et al. [15] found over Ni/A_2O_3 catalyst a much smaller value which might be due to several reasons, the presence of extraneous effects (diffusion of mass and heat in catalyst particle and mixing in the reactor), the lower range of temperature, hence a different rate determined step, and last but not least the absence of water in which these experiments were carried out. Akande et al. [17] also reported a much lower activation energy assuming Eley Rideal type kinetic model. Experiments in this latter work were carried out over Ni/Al_2O_3 catalyst under concentrated conditions where, in contrast with the intrinsic kinetic data assumed, diffusion of mass and heat in catalyst particle as well as mixing in the reactor are most likely to be limiting the rate of reaction.

4. Conclusions

Homogeneous precipitation method used in this work for synthesizing Ni(II)-Al(III) HDL precursors allows us to obtain, after reduction, catalysts with highly dispersed Ni in the alumina matrix. The H_2 production from ethanol steam reforming reached 5 mol H_2 per mol ethanol fed. The only products obtained were CO, CO_2, CH_4 and H_2, even for ethanol conversions lower than 100%. A set of two reactions in parallel was found to represent well the reaction system under diluted conditions. Both equations have a reaction order with respect to ethanol concentration lower than 1. It was verified that for each temperature of reaction there exists an ethanol/water molar ratio that maximizes the reaction rates. This behavior provides evidence that both reactants are adsorbed on the catalyst and they are competing for the same type of active site. Furthermore, experiments adding methane to the feed showed that methane is also adsorbed on the same active site. This idea is compatible with a Langmuir-Hinshelwood-type mechanism with only one type of active site. Thus, it is intended to complete this kinetic study adding to the fitting the experimental results using methane in the feed and assuming a Langmuir-Hinshelwood-type mechanism.

Acknowledgments

To Mr. Roberto Tejeda for TPR measurements. To University of Buenos Aires, CONICET and ANPCYT for the financial support.

References

[1] J. Llorca, N. Homes, J. Sales, P. Ramírez de la Piscina, J. Catal. 209 (2002) 306.
[2] J. Llorca, P. Ramírez de la Piscina, J.A. Delmon, J. Sales, N. Homes, Appl. Catal. 43 (2003) 355.
[3] S. Cavallaro, V. Chiodo, S. Freni, N. Mondillo, F. Frusteri, Appl. Catal. 249 (2003) 119.

[4] D.K. Liguras, D.I. Kondarides, X.E. Verykios, Appl. Catal. B Environ. 43 (2001) 345.
[5] B. Zhang, X. Tang, Y. Li, W. Cai, Y. Xu, W. Shen, Catal. Commun. 7 (2006) 367.
[6] P.D. Vaidya, A. Rodrigues, Chem. Eng. J. 117 (2006) 39.
[7] J.R.H. Ross, M.C.F. Steel, A. Zeini-Isfahani, J. Catal. 52 (1978) 280.
[8] J.R.H. Ross, M.C.F. Steel, J. Chem. Soc. Faraday I 69 (1973) 10.
[9] M. Marquevich, F. Medina, D. Montané, Catal. Commun. 2 (2001) 119.
[10] A. Corma, F. Melo, N. Morlanés, Actas XIX Simp. Iberoam. Cat. Mexico, 2001, p. 1166.
[11] F. Aupretre, C. Descorme, D. Duprez, D. Casanave, D. Uzio, J. Catal. 233 (2005) 464.
[12] A. Akande, R. Idem, A. Delai, Appl. Catal. A Gen. 287 (2005) 159.
[13] M. Belloto, B. Rebours, O. Clause, J. Lynch, D. Bazin, E. Elkaim, J. Phys. Chem. 100 (1996) 8535.
[14] D.A. Morgenstern, J.P. Fornango, Energy Fuels 19 (2005) 1708.
[15] J. Sun, X.-P. Qiu, F. Wu, W.-T. Zhu, Int. J. Hydrogen Energy 30 (2005) 437.
[16] P.D. Vaidya, A. Rodrigues, Ind. Eng. Chem. Res. 45 (2006) 6614.
[17] A. Akande, A. Aboudheir, R. Idem, A. Delai, Int. J. Hydrogen Energy 31 (2006) 1707.
[18] D.R. Sahoo, S. Vajpai, S. Patel, K.K. Pant, Chem. Eng. J. 125 (2007) 139.
[19] V. Mas, M.L. Dieuzeide, M. Jobbágy, G. Baronetti, N. Amadeo, M. Laborde, Catal. Today, in press.
[20] G.F. Froment, K.B. Bishoff, Chemical Reactor Analysis and Design, Wiley, New York, 1990.
[21] J.R. Rostrup-Nielsen, J. Sehested, J. Norskov, Adv. Catal. 47 (2002) 65.
[22] J. Comas, F. Mariño, M. Laborde, N. Amadeo, Chem. Eng. J. 98 (2004) 61.
[23] V. Mas, R. Kipreos, N. Amadeo, M. Laborde, Int. J. Hydrogen Energy 31 (1) (2006) 2.
[24] J. Comas, M. Dieuzeide, G. Baronetti, M. Laborde, N. Amadeo, Chem. Eng. J. 118 (2006) 11.
[25] J. Xu, G.F. Froment, AIChE J. 35 (1989) 88.